ISSN 0040-5795, Theoretical Foundations of Chemical Engineering, 2015, Vol. 49, No. 5, pp. 585–591. © Pleiades Publishing, Ltd., 2015.
Original Russian Text © E.A. Dmitriev, V.A. Kolesnikov, A.M. Trushin, V.A. Brodskii, R.B. Komlyashev, 2015, published in Teoreticheskie Osnovy Khimicheskoi Tekhnologii, 2015, Vol. 49, No. 5, pp. 489–495.

Some Hydromechanical Aspects of Microflotation

E. A. Dmitriev, V. A. Kolesnikov, A. M. Trushin, V. A. Brodskii, and R. B. Komlyashev

Mendeleev Russian University of Chemical Technology, Miusskaya pl. 9, Moscow, 125047 Russia

e-mail: rareran@mail.ru

Received January 26, 2015

Abstract—Some hydromechanical aspects of the generation of a dispersed gas phase by the electrochemical method and with tubular microfiltration membranes under the action of liquid phase inertia and the hindered motion of gas particles in the gravity field are considered as they apply to microflotation. Experimentally verified equations for calculating the average diameter of spherical gas bubbles and the velocity of their hindered motion are proposed.

Keywords: microflotation, electroflotation, compression microflotation, hydromechanical processes, generation of microbubbles, tubular microfiltration membranes, gas content, hindered motion

DOI: 10.1134/S0040579515050218

INTRODUCTION

The development of flotation as an engineering process was associated first of all with the purification of minerals and the beneficiation of ores. Ground (to nearly 0.3 mm) metal ores and some nonmetallic minerals are treated with flotation reagents, which enable the surface of particles to adhere to gas bubbles. Entraining solid particles, the latter move upward and are removed with a foam. For these purposes, flotation machines are units in which a ground ore is converted into an aqueous suspension with a solid phase content of 15–30 wt % by means of mechanical and/or air stirring. Nontarget minerals are not floated and remain in the lower section.

Due to solving the urgent environmental protection problem, in particular, of liquid technogenic waste purification, and the water purification and treatment problems, flotation was further developed as an engineering process for the purification of liquid media with a small concentration of solid or liquid particles in a dispersion. In this case, a dispersed gas phase is obtained in the process of microflotation as an ensemble of bubbles with sizes of 10–140 μm and a gas content of up to 10% due to the small sizes of the removed particles.

GAS-PHASE DISPERSION

The generation of microbubbles in the process of microflotation is usually performed by electrochemical or compression methods. In the first case, this is generally accomplished using insoluble electrodes (electroflotation process). In the second case, a gas is converted into a dispersed phase using different porous materials (compression microflotation).

The electroflotation process is based on water electrolysis, which, as a rule, generates a gas flow of hydrogen and oxygen on stainless steel cathodes and titanium based anodes with a conductive oxide coating [1]. Compression flotation can be implemented by means of ceramic, glass, or metallic membranes [2, 3].

In the process of electroflotation, the bubble sizes and gas content are controlled by selecting the curvature of electrodes and the electrical current density. Thus, a cathode 1.5 mm in diameter evolves hydrogen bubbles 40–120 μm in size, while a cathode 0.4 mm in diameter generates bubbles of 20–40 μm in size [1]. The authors [1] propose determining the number of hydrogen bubbles per unit dispersion volume from the relationship

$$N = \frac{6A_e\tau i}{\pi d^3 \rho_G h_F}, \quad (1)$$

where A_e is the electrochemical equivalent of hydrogen, kg/(A s); τ is the electroflotation time, s; d is the bubble diameter, m; ρ_G is the hydrogen density, kg/m^3; h_F is the height of a treated liquid layer above the electrode assembly, m; $i = I/S$ is the cathode current density, A/m^2; I is the current strength, A; and S is the horizontal cross section area of a unit, m^2.

Moreover, the size of gas bubbles is affected by the composition of the electrolyte, the pH of a medium, the presence of surfactants, and other factors.

When a gas phase is dispersed using membranes, the sizes of the gas bubbles depend not only on the sizes of membrane pores, but also on the character of bubbling, i.e., into a quiescent or moving liquid phase. In the case of bubbling into a quiescent liquid, the size

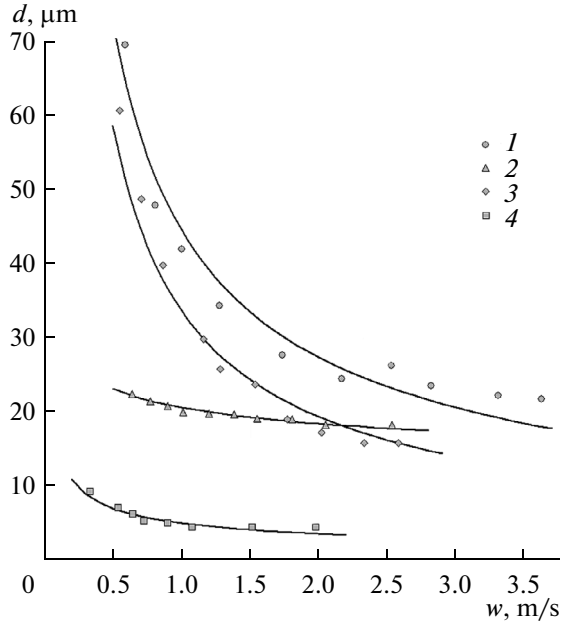

Fig. 1. Diameter of formed microbubbles versus average liquid (water) velocity in a membrane channel: (*1*) ceramic membrane with d_0 = 2.6 μm and an inner diameter of 6 mm [5], (*2*) glass membrane with d_0 = 2.23 μm and an inner diameter of 5.6 mm [6], (*3*) ceramic membrane with d_0 = 0.5 μm [5], (*4*) glass membrane with d_0 = 0.55 μm [6] (solid lines *1*–*4* were plotted by Eq. (2)).

of microbubbles proves to be several times greater than for bubbling into a moving liquid phase [4]. In the case of a liquid phase flowing over a membrane, the liquid inertia force produces a major effect on the mechanism of microbubble detachment. We have proposed a mathematical model for the formation of microbubbles upon the dispersion of a gas through the pores of microfiltration membranes [5]. The model is based on the balance of friction forces appearing under the action of inertia from a moving liquid phase, surface tension forces, and normal forces of mutual pressure between formed microbubbles. Due to the small sizes and the presence of surfactants in the liquid, the bubbles have a hindered surface. For this reason, the hydraulic friction coefficient is determined considering an ensemble of surface bubbles as a granular asperity. The buoyant force has not been taken into account due to its smallness in comparison with the above listed forces. As a result, the relationship obtained for the average diameter of microbubbles d is as follows:

$$d = \left[\frac{\sigma d_0\left(16\lambda\rho_L w^2 + 64\pi K w^n\right)}{\left(\lambda\rho_L w^2\right) + 64\left(K w^n\right)^2}\right]^{\frac{1}{2}}, \qquad (2)$$

where σ is the surface tension, N/m; d_0 is the average diameter of membrane pores, m; λ is the hydraulic friction coefficient; ρ_L is the liquid phase density, kg/m^3; w is the average liquid velocity in a channel, m/s; and K and n are empirical constants.

Hence, the diameter of formed microbubbles depends on the surface tension and density of a liquid phase and the sizes of membrane pores and depends in a complex manner on the average flow velocity in a tubular membrane channel. Moreover, the empirical coefficients K and n depend on the porosity of a membrane, the roughness of its surface, and the size distribution of membrane pores.

The obtained relationship was verified by our experiments [5] and the data of other authors [6] for tubular ceramic and glass within a range of average liquid (water and aqueous solutions) velocities of 0.5–3.5 m/s. It has been found that the deviation of theoretical curves from experimental results is less than 8.6%. Some typical curves are plotted in Fig. 1. A common regularity for ceramic and glass membranes is a strong dependence between the size of formed microbubbles and the liquid velocity in a channel at low velocities (0.5–1 m/s) and a very weak dependence between these parameters at comparatively high velocities. At velocities above 2 m/s corresponding to the Reynolds number Re > 12000, the diameter of bubbles becomes almost independent of the liquid phase velocity.

The analysis of the obtained data shows that the coefficient K has rather close values for ceramic membranes with different pore diameter, whereas the power n for a membrane with an average pore diameter d_0 = 0.5 μm is several times lower than for a membrane with d_0 = 2.6 μm. This can be explained by the fact that the roughness asperities of ceramic membranes shield bubbles of small diameter, which decrease their force, the effect of which is intensified by the friction force on large bubbles. A similar effect of decreasing the action of inertia on microdrops due to the influence of roughness is discussed in work [7] devoted to the preparation of emulsions using ceramic membranes. The reduction of the effect of friction force with a decreasing size of microbubbles also confirms that the growth of small bubbles (<20 μm) occurs inside the laminar sublayer, where the liquid velocity is low and changes slightly with increasing velocity in the flow core. The effect of roughness on the average diameter of bubbles is especially appreciable when comparing the experimental data obtained on ceramic and glass membranes (Fig. 1). The diameters of microbubbles obtained on relatively rough ceramic and smooth glass membranes with great pores (curves *1* and *2*, respectively) differ from each other much less than for membranes with small pores (curves *3* and *4*).

It is noteworthy that the information on the average diameter of microbubbles is insufficient for a detailed description of hydrodynamic processes occurring in flotation and electroflotation, and the literature data on the size distribution of microbubbles are scanty.

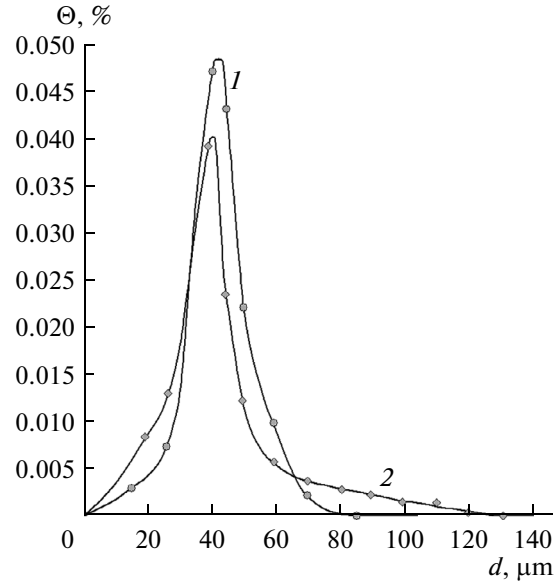

Fig. 2. Differential function of the size distribution of hydrogen bubbles generated on a nickel cathode at a current density of (*1*) 50 and (*2*) 200 A/m^2.

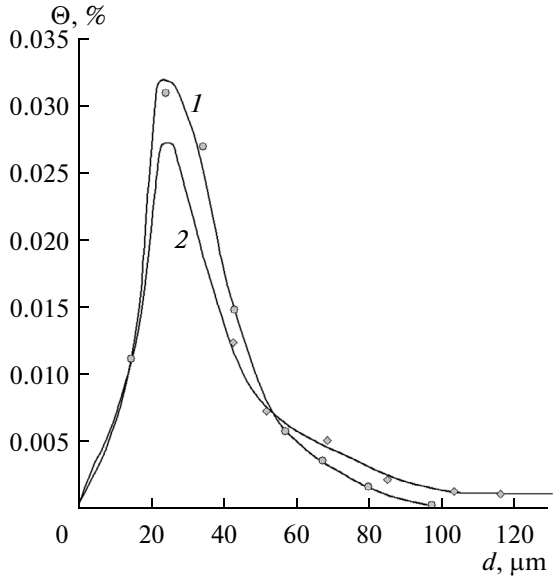

Fig. 3. Differential function of the size distribution of hydrogen bubbles generated on a zinc cathode at a current density of (*1*) 50–150 and (*2*) 250 A/m^2.

The integral functions obtained for the size distribution of hydrogen bubbles at different current densities on nickel and zinc cathodes are given in [1]. The differential curves in Figs. 2 and 3 were obtained from the integral distributions [1]. As shown by the performed studies, more uniform bubbles with diameters of 35–50 μm are typical of the nickel-based cathode, whereas their great polydispersity with a range of variations of 15–70 μm is observed for the zinc cathode. The presence of soluble and insoluble admixtures in water can have some effect on the disperse composition of the gas phase. As a rule, admixtures decrease the size of bubbles and stabilize a gas–liquid dispersion. It has been revealed that hydroxides of metals (Fe^{3+}, Cr^{3+}, Cu^{2+}, Ni^{2+}, Zn^{2+}) have a rather great stabilizing effect, which can explain the rather good floatability of these compounds. The introduction of a surfactant into a solution, in particular A-40 and KMN, inhibits coalescence and enables the generation of finely dispersed gas bubbles, which form a large gas–liquid phase interface. These bubbles, which float up at very low velocities, have a considerable time of contact with floated particles and therefore increase the efficiency of flotation. Hence, the process of microflotation can be managed by varying the chemical composition of treated sewage water to specify the gas content and control the size of bubbles.

Some typical differential curves for the size distribution of microbubbles generated via the dispersion of a gas through tubular ceramic membranes under the action of liquid phase inertia are plotted in Figs. 4 and 5. As can be seen from Figs. 4 and 5, the size of bubbles varies from 10 to ~200 μm for the membrane with a pore diameter $d_0 = 2.6$ μm and from 5 to ~140 μm for the membrane with a pore diameter $d_0 = 2.6$ μm. In this case, the average diameter of bubbles is reduced with a decrease in the size of membrane pores and an increase in the liquid velocity in a channel, thus being in complete agreement with Eq. (2).

Hence, the generation of microbubbles with a corresponding size distribution can be performed by both the electrochemical method and the dispersion

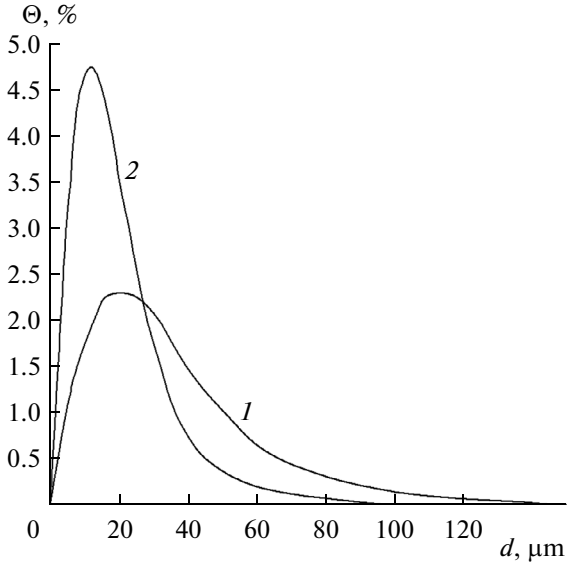

Fig. 4. Differential size distribution of microbubbles generated on ceramic membranes with an average pore diameter of 2.6 μm at a liquid velocity in a channel of (*1*) 1.02 and (*2*) 2.82 m/s.

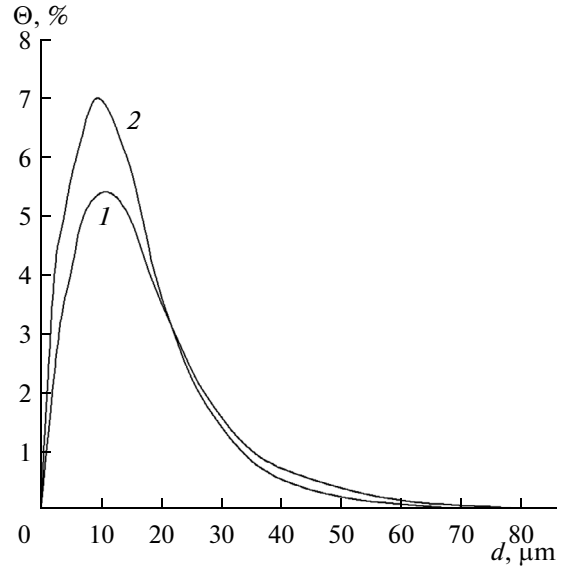

Fig. 5. Differential size distribution of microbubbles generated on ceramic membranes with an average pore diameter of 0.5 μm at a liquid velocity in a channel of (*1*) 0.78 and (*2*) 2.05 m/s.

through microporous membranes under the action of liquid phase inertia. In both cases, it is possible to control the gas content and the disperse composition of the gas phase.

HINDERED MOTION OF SPHERICAL GAS PARTICLES IN A LIQUID IN THE GRAVITY FIELD

The second but no less important hydrodynamic aspect in the consideration of microflotation is the motion of spherical gas particles in a great volume of liquid in the gravity field. This motion becomes hindered, even at comparatively small gas contents (5–10%).

In microflotation practice, the velocity of the hindered laminar motion of microbubbles is determined using the Happel equation derived for the motion of solid spheres from the cellular model, i.e.,

$$v = v_0\left[\frac{3 - 4.5\left(\varphi^{1/3} + \varphi^{5/3}\right) - 3\varphi^2}{3 + 2\varphi^{5/3}}\right]. \quad (3)$$

This equation is applied for microbubbles floating upward in the Stokes regime at $\mathrm{Re} < 2$. However, it can also be used at $2 < \mathrm{Re} < 40$ [8]. For electroflotation at a low gas content (below 5%), it is proposed to use the simpler formula

$$v = v_0\left(1 - 1.5\varphi^{1/3}\right). \quad (4)$$

In Eqs. (3) and (4), v is the velocity of the hindered motion of a disperse phase particles, m/s, v_0 is the velocity of a single particle, m/s, and φ is the gas content.

For the turbulent motion of spherical bubbles in pure liquids in the region of $40 < \mathrm{Re} < 400$, it is recommended [9] to use the equation derived from the cellular model by Marrucci [10], i.e.,

$$v = v_0\left[\frac{(1-\varphi)^2}{1-\varphi^{5/3}}\right]. \quad (5)$$

The velocity of the hindered motion of solid and gas particles is also often determined in the literature using the empirical formula [11]

$$f_e(\varphi) = \frac{v}{v_0} = (1-\varphi)^n. \quad (6)$$

The power n for the motion of spherical gas particles depends on the Morton number (M) and the Reynolds number (Re_p). There are few literature data on the estimation of the rise velocity of gas bubbles in the hindered regime. When using Eq. (6) in calculations, it is usually assumed that $n = 1.75–2$.

A typical feature of Eqs. (3)–(6) that describe the hindered motion of particles is the assumption about a uniform distribution of dispersed particles over the volume of a layer. It should be noted that this assumption contradicts numerous experimental data on the motion of both gas and solid particles in a liquid.

We have developed a mathematical model for estimating the velocity of the hindered motion of spherical gas particles [12] on the basis of minimum energy dissipation intensity with allowance for a non-uniform concentration distribution of dispersed phase particles over the cross section of an apparatus. The rigorous analytical solution of this problem is impossible due to the complexity of its mathematical description, so the energy dissipation intensity was written in a slightly simplified form.

Considering the hindered motion of dispersed particles in a column filled with a liquid and introducing the velocity of the motion of particles relative to the liquid $v_{rel} = v_b/[\varphi(1-\varphi)]$ and the vertical walls of an apparatus $v = v_b/\varphi$, we have

$$v_{rel} = \frac{v}{1-\varphi}. \quad (7)$$

The ratio of hindered and free motion velocities in this region is a function of the dispersed phase content to be determined, i.e.,

$$\frac{v}{v_0} = f(\varphi). \quad (8)$$

The resistance force F of a spherical gas particle with a diameter d is written as

$$F = \lambda\frac{v_{rel}^2}{2}\rho_L\frac{\pi d^2}{4} = \lambda\frac{v_0^2 f^2(\varphi)}{2(1-\varphi)^2}\rho_L\frac{\pi d^2}{4}. \quad (9)$$

Then, the dissipation of energy during the motion of a single particle can be written as

$$\Phi_0 = F_V = \lambda \frac{v_0^3 f^3(\varphi)}{2(1-\varphi)^2} \rho_L \frac{\pi d^2}{4}. \quad (10)$$

When particles float up in a group (cloud), they occupy a certain part of the cross section S_1 of the total cross section of an apparatus S. Hence, $\varphi_{tr} S_1 = \varphi S$, where φ_{tr} is the true dispersed phase content.

The number of particles N in a layer with a height H is $N = 6H\varphi_{tr} S_1/(\pi d^3)$, and the volume of liquid in a layer filled with particles is $V = HS_1(1 - \varphi_{tr})$. In this case, the intensity of energy dissipation per unit volume is

$$\Phi = \frac{\Phi_0 N}{V} = \frac{3}{4}\frac{\lambda}{d} \frac{\rho_L v_0^3 f^3(\varphi)\varphi_{tr}}{2(1-\varphi)^2(1-\varphi_{tr})}. \quad (11)$$

Taking the resistance coefficient in the form $\lambda = A/(\mathrm{Re}_r^m)$, where $\mathrm{Re}_r = vd/[(1 - \varphi)\nu]$, with a certain degree of approximation, we obtain

$$\Phi = \frac{3}{4} \frac{A\rho_L \nu^m v_0^{3-m} f^{3-m}(\varphi)\varphi_{tr}}{d^{m+1} 2(1-\varphi)^{2-m}(1-\varphi_{tr})}. \quad (12)$$

As mentioned in [12], parameter A depends on the dispersed phase content at a constant power m due to the intensification of interaction between dispersed particles with an increase in their concentration.

For the hindered motion of a spherical gas particles considered as extraneous, the balance of the forces acting on it has the form

$$\lambda \frac{\rho_L}{d} \frac{v_0^2 f_e^2(\varphi)}{(1-\varphi)^2} \frac{\pi d^2}{4} = (\rho_L - \rho_G) \frac{\pi d^3}{6} g(1-\varphi). \quad (13)$$

Expressing parameter A as the product of A_1 that is constant for this region and a certain function $f_1(\varphi)$, we have

$$\frac{A_1 f_1(\varphi) f_e^{2-m}}{(1-\varphi)^{3-m}} = \frac{4}{3} \frac{(\rho_L - \rho_G) g d^{m+1}}{\rho_L v_0^{2-m} \nu^m}. \quad (14)$$

Since the right part of Eq. (14) does not depend on φ, we obtain

$$f_1(\varphi) = \frac{(1-\varphi)^{3-m}}{f_e^{2-m}(\varphi)},$$

$$A_1 = \frac{4}{3} \frac{(\rho_L - \rho_G) g d^{m+1}}{\rho_L v_0^{2-m} \nu^m}.$$

In compliance with Eq. (6), $f_1(\varphi)$ is also a power function $ff_1(\varphi) = (1 - \varphi)^{n_1}$; hence,

$$(1-\varphi)^{n_1} = \frac{(1-\varphi)^{3-m}}{(1-\varphi)^{n(2-m)}}.$$

From the last equation, we have

$$n_1 = 3 - m + n(m-2). \quad (15)$$

Taking into account that the resistance coefficient for the hindered motion of spherical bubbles in pure liquids is usually inversely proportional to Re_r ($m = 1$), and the power n is close to 2 at both small and rather high Re_r, the power n_1 determined from Eq. (15) is close to zero, i.e., the preformed analysis demonstrates the independence of A from the gas content. However, it should be taken into account that the hindered motion velocity depends on the gas content and, consequently, the presence of even trace surfactants in the liquid has an effect on the power n. Hence, the further assumed constancy of the parameter A should be considered as approximate, i.e., as a certain averaged value within the considered gas content range.

The presence of the average (φ) and true (φ_{tr}) disperse phase content in Eq. (12) is due to fluctuations in the concentration of the dispersed phase produced by the displacement of particles along the flow cross section. Taking into account the growth in the relative fluctuation value with an increase in the reciprocal dispersed phase content [12], we obtain

$$\varphi_{tr} = a + \varphi(1 + b). \quad (16)$$

Since the difference between φ_{tr} and φ decreases with increasing φ, the constant b will be negative and, taking into account that the dispersed phase content may not exceed 0.62 for monodispersed randomly packed spherical particles, the constraint imposed on Eq. (16) is as follows:

$$a + \varphi(1 + b) \le 0.62. \quad (17)$$

It follows from Eq. (12) that the intensity of energy dissipation per unit liquid volume depends on the physicochemical properties of a system (density of phases, viscosity, diameter of dispersed phase particles) and the dispersed phase content. The first group of parameters is governed by the nature of phases, pressure, temperature, and the design of a dispersing device, i.e., specified by external conditions. Then, the only independent variable that determines the self-organizing ability of a system is the dispersed phase content.

In view of the aforesaid, it is necessary to write Eq. (12) in the form

$$\Phi = BF(\varphi), \quad (18)$$

where $B = \frac{3}{4} \frac{A\rho_L \nu^m v_0^{3-m}}{d^{m+1}}$, $F(\varphi) = \frac{f^{3-m}(\varphi)\varphi_{tr}}{(1-\varphi)^{2-m}(1-\varphi_{tr})}$.

The steady state of this system (layer consisting of spherical particles moving in a continuous phase) corresponds to the minimum intensity of energy dissipation. This condition corresponds to an extremum of the functional

$$I(\varphi) = \int_V \Phi dV = \int_V BF(\varphi) dV. \quad (19)$$

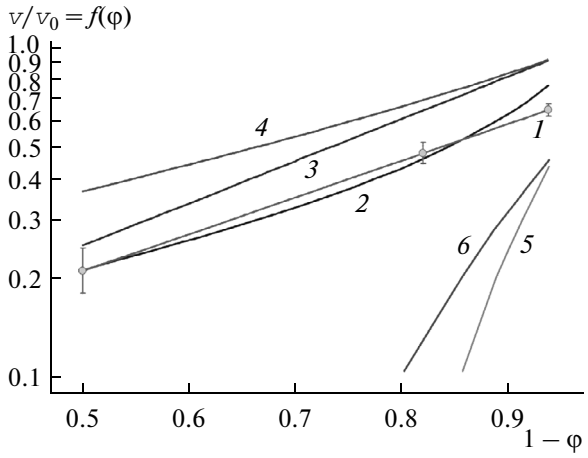

Fig. 6. Ratio of the hindered and free motion velocities of spherical bubbles versus dispersed phase content (Ar = 300): (*1*) experimental data with a spread field, (*2*) Eq. (20), (*3*) Eq. (6) at $n = 2$, (*4*) Eq. (5), (*5*) Happel equation (3), (*6*) Eq. (4).

An extremum of functional (19) corresponds to its steady-state value

$$\delta \int_V BF(\varphi)\, dV = 0.$$

Since the variation operation is permutative with the integration operation,

$$\delta \int_V BF(\varphi)\, dV = \int_V \delta\left[BF(\varphi)\right] dV = 0.$$

Due to the randomness of the volume V, the subintegral expression is zero, i.e.,

$$\delta\left[BF(\varphi)\right] = \delta B + \delta F(\varphi) = 0.$$

Since $\delta B = 0$, $\delta F(\varphi) = 0$, i.e., the set of parameters under the variation sign is equal to a certain constant

$$c = \frac{f^{3-m}(\varphi)\,\varphi_{tr}}{(1-\varphi)^{2-m}(1-\varphi_{tr})}.$$

Hence, the ratio of hindered and free motion velocities with allowance for Eq. (16) has the final form

$$\frac{v}{v_0} = f(\varphi) = \left\{\frac{c(1-\varphi)^{2-m}\left[1-a-\varphi(1+b)\right]}{a+\varphi(1+b)}\right\}^{\frac{1}{3-m}}. \quad (20)$$

The constant c can be determined using the boundary condition of equal hindered and free motion velocities at a dispersed phase content tending to zero $f(0) = 1$ and, in this case, $c = a/(1-a)$. However, this boundary condition requires the coupled motion of particles at low φ, which is only possible at small sizes of particles when the distances between them are rather short due to their great number even at low φ. It should be noted that this state is typical for microflotation processes. In the general case, the constant c can be found using experimental $f_e(\varphi)$, if experimental data are available.

As for the coefficient m, as already mentioned above, it can be assumed to be 1.

In the calculation of $f(\varphi)$ by Eq. (20), the coefficient a was taken equal to 0.06–0.07 in all the cases, and the coefficient b was −0.1 in compliance with constraint (17).

The equations recommended for the calculation of the ratio of hindered and free motion velocities $v/v_0 = f(\varphi)$ and the experimental data [12] are compared in Fig. 6. As follows from Fig. 6, the values of $f(\varphi)$ calculated by proposed equation (20) are closest to the experimental data. Empirical relationship (6) with $n = 2$ and Eq. (5) derived based on the cellular model by Marrucci [10] yield obviously overestimated results. As for Happel equation (3) and relationship (4) derived from it, we observe the opposite picture; the calculated values of $f(\varphi)$ are strongly underestimated compared with the experimental data, even in the region of small φ.

CONCLUSIONS

The studies of hydromechanical processes that occur in the generation of a dispersed gas phase by the electrochemical method and with tubular microfiltration membranes as applied to microflotation show that it is possible to control the gas content and the disperse composition of the gas phase in both cases. This is accomplished by varying the electrical current density and the curvature of electrodes in the first case and by adjusting the liquid velocity in a channel and the gas feed velocity in the second case.

The analysis of the relationships recommended for calculating the hindered motion velocity of spherical gas particles in a liquid in the gravity field shows that the equation derived based on the variation principle of minimum energy dissipation intensity satisfactorily describes the experimental data within a dispersed phase content range of 0–0.5.

The obtained results are recommended for use when calculating microflotation processes.

ACKNOWLEDGMENTS

This work was supported by the Russian Scientific Foundation (project no. 14-29-00194) and the Russian Foundation for Basic Research (project no. 13-03-00528).

NOTATION

A_e—electrochemical equivalent of hydrogen, kg/(A s);

d—average diameter of particles, m;

d_0 —average diameter of membrane pores, m;

$f(\varphi)$ —gas content function;

$f_e(\varphi)$ —empirical gas content function;

g —gravity acceleration, m/s^2;

H —layer height, m;

m —constant defined over the entire given region of motion;

N —number of particles in a layer;

V —volume of liquid in a layer, m^3;

v —hindered motion velocity of dispersed phase particles, m/s;

v_0 —hindered motion velocity of dispersed phase particles, m/s;

w —average velocity of the liquid phase in a channel, m/s;

λ —resistance coefficient;

μ —dynamic liquid viscosity, Pa s;

ν —kinematic liquid viscosity, m^2/s;

ρ_G—gas phase density, kg/m^3;

ρ_L —liquid phase density, kg/m^3;

σ —surface tension, N/m;

Φ —energy dissipation intensity, W/m^2;

φ —average dispersed phase content;

φ_{tr}—true dispersed phase content;

Ar—Archimedes number;

Re—Reynolds number for a liquid flow in a channel;

Re_r—Reynolds number for a spherical gas bubble.

REFERENCES

1. *Elektroflotatsionnaya tekhnologiya ochistki stochnykh vod promyshlennykh predpriyatii* (Electroflotation Technology of Industrial Wastewater Treatment), Kolesnikov, V.A., Ed., Moscow: Khimiya, 2007.
2. Rodrigues, R.T. and Rubio, J., New basis for measuring the size distribution of bubbles, *Miner. Eng.*, 2003, vol. 16, pp. 757–765.
3. Yoon, R.-H., Microbubble flotation, *Miner. Eng.*, 1993, vol. 6, pp. 619–630.
4. Kukizaki, M. and Goto, M., Spontaneous formation behavior of uniform-sized microbubbles from Shirasu-porous-glass (SPG) membranes in the absence of water-phase flow, *Colloids Surf., A*, 2006, vol. 296, pp. 174–181.
5. Trushin, A.M., Dmitriev, E.A., and Akimov, V.V., Mechanics of the formation of microbubbles in gas dispersion through the pores of microfiltration membranes, *Theor. Found. Chem. Eng.*, 2011, vol. 45, pp. 26–32.
6. Kukizaki, M. and Goto, M., Size control of nanobubbles generated from Shirasu-porous-glass (SPG) membranes, *J. Membr. Sci.*, 2006, vol. 281, pp. 386–396.
7. Schröder, V., Behrend, O., and Schubert, H., Production of emulsions using microporous ceramic membranes, *Colloids Surf., A*, 1999, vol. 152, pp. 103–109.
8. Rulev, N.N., Collective velocity of bubbles floating up, *Kolloidn. Zh.*, 1977, vol. 39, no. 1, pp. 80–86.
9. Deryagin, B.V., Dukhin, S.S., and Rulev, N.N., *Mikroflotatsiya: Vodoochistka, obogashchenie* (Microflotation: Water Purification and Enrichment Processes), Moscow: Khimiya, 1986.
10. Marrucci, G., Rising velocity of a swarm of spherical bubbles, *Ind. Eng. Chem. Fundam.*, 1965, vol. 4, no. 2, pp. 224–225.
11. Coulson, J.M., Richardson, J.F., Backhurst, J.R., and Harker, J.H., *Coulson and Richardson's Chemical Engineering*, vol. 2: *Particle Technology and Separation Processes*, Oxford: Butterworth–Heinemann, 1991.
12. Trushin, A.M., Dmitriev, E.A., Nosyrev, M.A., Tarasova, T.A., and Kuznetsova, I.K., Determining the velocity of the hindered motion of spherical gas particles through liquid in a gravity field, *Theor. Found. Chem. Eng.*, 2013, vol. 47, pp. 368–374.

Translated by E. Glushachenkova